

Supplemental Information for:

Mesoscale Blood Cell Sedimentation for Rapid Collection of Millilitre Samples†

C. Galligan^a, J. Nichols^b, E. Kvam^c, P. Spooner^c, R. Gettings^b, L. Zhu^b, and C. M. Puleo^a

S1- Addendum to Experimental Methods

Device Fabrication: Figure S1 shows the component pieces used to assemble the plasma separation device. Three rapid prototyped parts (Top Chambers, Sedimentation Chamber, and Bottom; Fineline Prototyping, Watershed Polymer, USA) were assembled using pressure sensitive adhesive films (3M VHB, 100 μm , USA). Before assembly, the VHB adhesive film was cut to the proper profiles with a Graphtec Cutting Pro FC4500-50 cutting plotter (Graphtec America, USA). The pressure sensitive adhesive formed a perimeter seal around the microchannel, and allowed for fluidic connection between the three main chambers (whole blood inlet, sedimentation, and plasma collection). The microporous membrane was placed over the sedimentation chamber and was bonded to the device using the adhesive films. Once fully assembled, a table top heated press was used to setup the pressure sensitive adhesive and ensure sealing. An access hole built into the sedimentation chamber was used to prime the device with isotonic buffer; an adhesive metal foil film was then applied to the chamber ports creating a fully enclosed device that was stored until use. For experiments, the metal foil covering on the whole blood input chamber was removed, and the chamber was then loaded with 0.5 – 1 mL whole blood (Bioreclamation, USA). An access port built into the top wall of the plasma collection chamber was then attached to a vacuum source (either a hand-actuated or syringe pump mounted syringe). Upon drawing vacuum, whole blood was pulled across the microporous membrane (covering the sedimentation chamber), cells were captured within the sedimentation chamber, and plasma was drawn into the collection chamber. An excess 0.5 mL of buffer was then drawn across the collection chamber to ensure that the majority of the plasma components were collected (termed Post-blood Flushing Buffer below). During this process, cells remained trapped in the sedimentation chamber. Once this was complete, the metal foil covering the plasma collection chamber was removed, and plasma was collected for analysis using a pipette.

Sample Collection: Needle ports were glued into both the sedimentation and plasma collection chamber. These ports were sealed during device operation using heat-sealed tygon tubing. These removable seals enabled post-operation collection of 1) sedimented cells within the sedimentation chamber and 2) cell-free plasma within the plasma collection chamber. In addition, after operation of the device, the foil seal over the plasma collection chamber (which enabled vacuum operation of the device) could be removed and plasma could be collected with as simple pipette.

Measuring Cell Capture Efficiency: In order to measure the cell capture efficiency of the device leukocyte counts were established for the input whole blood, the fluid within the sedimentation chamber, and fluid within the plasma collection chamber. Cell counts were measured using a Sysmex poch automated Hematology Analyzer, and cell capture efficiency was expressed as the percent of total

cells contaminating the plasma collection chamber. Additional red blood cell data (not shown) also showed near 100% capture of RBCs within the sedimentation chamber. Figure S2 shows the device in use in a step-by-step chart, including collection of the cells and plasma in two separate compartments.

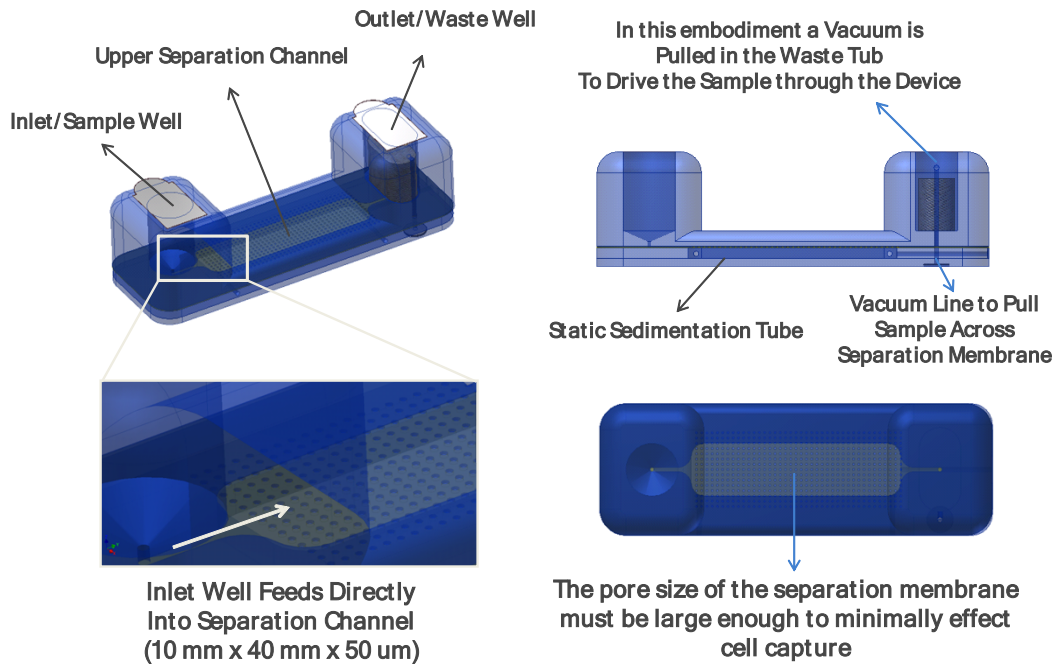


Figure S1. Further detail of the mesoscale sedimentation device, showing the device components and sections (seems within the device represent layers that were laminated to create the final device).

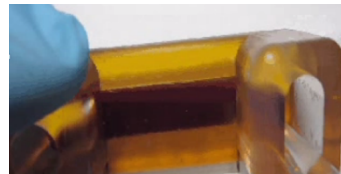
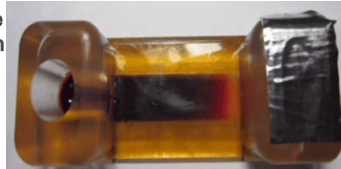
Step One - 0.5 mL Whole Blood into Inlet Well



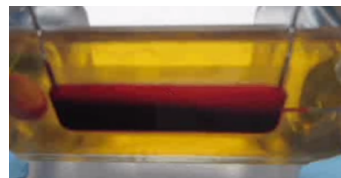
Step Two - Vacuum applied to waste chamber, sample begins movement through device



Step Three - Device runs until collection tub is filled with sedimented cells



Step Four - Only plasma has moved to the waste chamber, cells have efficiently settled to the collection tub



Step Five - Cells are visible in the collection tub from the bottom



Step Six - Collection tub may be opened and collected cells Drained from the device

Figure S2. Step-by-step images of the sedimentation device in use to collect both plasma and blood cells from 0.5 mL of blood in separate chambers.

S2 – Investigating Device Dimensions

Critical device dimensions vs operating parameters. A face-centered central composite design of experiment (DoE) was performed to evaluate device performance at variable critical height (h) and residence time (t_r). Multiple devices, 4 cm long x 1 cm wide, were assembled using inserts of 0.2, 0.4, and 0.6 cm yielding device volumes (V) between 750 to 2250 μL . A feed solution containing 0.04 w/v % 2 μm silica standard particles was prepared in deionized water and processed through the device at residence times of 240, 360, and 480 seconds. The flow rates (F) were calculated as follows: $F = V/t_r$. The turbidity of the feed solution was recorded before each run and pumped through the device at the calculated flow rates. Using the data obtained from the DoE runs, a transfer function for 2 μm particles was generated using MINITAB 12.23.

Basic design principle. A simple relationship between the critical height and residence time accounts for much of the performance variance in the device. As shown in figure 1 of the article text, the device can be optionally configured with and without both the microchannel at the inlet and outlet and the microporous membrane. The major performance governing dimension of the device is the height between the inlet and/or outlet and the floor of the collection chamber. This dimension is called the critical height and is the largest determinant of device performance. Highly efficient particle separation can be achieved when the critical height is matched to the settling characteristics of a particle.

A series of experiments were run to establish the relationship between the critical height and particle settling characteristics. The devices were configured to have a 4 x 1 cm collection chamber with varying depths, no microchannels, and no microporous sieves. A transfer function was established that accounts for 99.4% of the performance variability and determines the relationship between residence time and critical height for a monodisperse sample of 2 μm silica particles. The experimental results used to generate the transfer function and the regression statistics are shown in Table 1. A time to capture was calculated using Stoke's settling velocity and the critical height for each experiment. The capture time results can also be found in Table 1.

Estimated Regression Coefficients for Capture				
Term	Coef	StDev	T	P
Constant	0.4895	0.015609	31.362	0.000
depth	-0.1576	0.009012	-17.483	0.000
rT	0.0698	0.009012	7.748	0.004
depth*depth	0.1249	0.018024	6.932	0.006
depth*rT	-0.0854	0.011038	-7.737	0.004

S = 0.02208 R-Sq = 99.4% R-Sq(adj) = 98.5%

Transfer Function:
Y (particle capture) = 0.1249 (h²) - 0.854 (rT*h) + 0.0698 (rT) - 0.1576 (h) + 0.4895

RUN	Critical Height (cm)	V (cm ³)	t _R (sec)	F (mL/min)	Turbidity IN (NTU)	Turbidity OUT (NTU)	Expt. Particle Capture (%)	Capture Time (s)
1	0.60	2.4	480	0.30	656	364	45	1775
2	0.60	2.4	240	0.60	759	387	49	1775
3	0.20	0.8	480	0.10	679	58	91	600
4	0.60	2.4	360	0.40	822	464	44	1775
5	0.40	1.6	240	0.40	717	426	41	1183
6	0.20	0.8	240	0.20	534	204	62	600
7	0.40	1.6	480	0.20	717	306	57	1183
8	0.20	0.8	360	0.13	633	137	78	600

Table S1. Results from a 2x2 DoE for critical height and residence time.

The trend in capture efficiency mirrors the trend in capture time with respect to residence time. The highest capture efficiency occurs when the residence time is closest to the particle capture time at a given critical height (Run 3). Conversely, the worst efficiency occurs when the residence is much shorter than the theoretical particle capture time (Runs 1, 2, and 4). Additional factors contribute to particle capture in the device beyond particle settling physics including edge effects, dead volumes, variable device height as the collection chamber fills with sediment, inlet microchannel length, and the presence of a microporous sieve.

Improved capture with microchannels and microporous sieve. A number of experiments demonstrated the enhancements provided by incorporating both inlet/outlet microchannels and a microporous sieve. Capture efficiencies for 2 μm particles with various device configurations are presented in Table 2. The devices were configured to have a 4 x 1 x 0.2 cm collection chamber and were run at a residence time of 240 s. Microchannel lengths were varied at inlet and outlet between 0 and 66.5 mm. The presence of a 40 μm microporous mesh was also varied within the device. The baseline capture efficiency for a device with neither microchannels nor a microporous sieve was 60% (Entry 1). Adding an inlet microchannel with varying length resulted in increased capture efficiencies of up to 81% at the arbitrary limit set on device length (Entries 1-3). The presence of a microporous sieve also increased capture efficiencies up to 81% at the arbitrary limit set on device length (Entry 2 & 4).

Entry	Microchannel Length, mm (Inlet/Outlet)	Microporous Sieve (+/-)	Capture Efficiency (%)
1	0/0	-	60
2	16.5/16.5	-	71
3	66.5/16.5	-	81
4	16.5/16.5	+	81

Table S2. Comparison of particle capture efficiency for 2 μm particles between devices with and without both microchannels at the inlet/outlet and a microporous sieve over the collection chamber.

These initial results demonstrated that the microchannel and microporous mesh features may be utilized to increase blood cell capture efficiency (in a pre-determined manner), as shown in the article text.

S3 – Mesoscale Blood Sedimentation vs. Cell Filtration Membrane

In order to compare the capture efficiency of the cell sedimentation device to other separation technologies that may be useful in remote or point-of-care settings, we measured the number of white blood cells (WBCs) escaping capture in the sedimentation device and compared this to the performance of a leading depth filter designed for capture of WBCs. The percent of cells captured was determined by comparing the number of WBCs per mL of sample before and after separation (using the Sysmex blood analyzer), and the experiment was performed in triplicate. 0.5 mL blood samples were run through both devices at 250 $\mu\text{L}/\text{min}$. Figure S3 (A and B) shows that the mesoscale sedimentation chamber outperforms standard filtration techniques at these high flow rates. It is noteworthy that the capture efficiency demonstrated using the commercial filter required the use of 5 stacked filters (one filter only captured 26.2 % of the cells). The stacked depth filters showed a 1 mL dead volume, and did not allow easy collection of the captured cells. In contrast, figure S3C shows that capture efficiency in the mesoscale sedimentation chamber is maintained across a wide range of operating flow rates (50-1000 $\mu\text{L}/\text{min}$; blue bars). In addition, the sedimentation chamber could be flushed and the captured cells could be collected for further down-stream analysis with little loss (figure S3C; red bars).

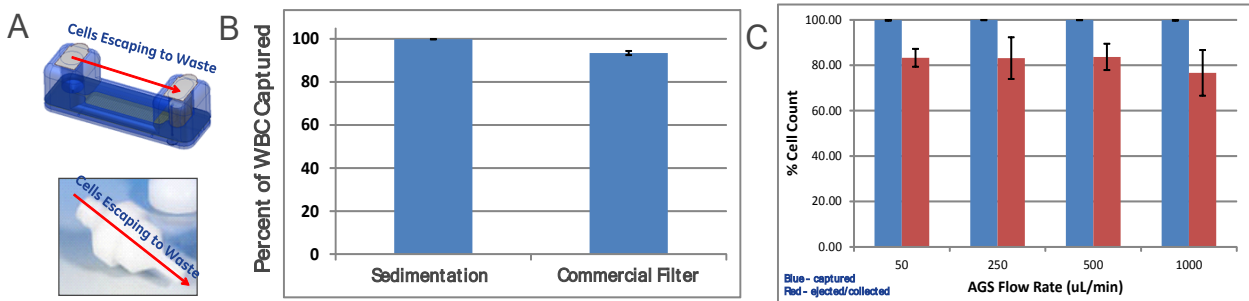


Figure S3. A. Depicts the experimental comparison of blood cells that escape capture in either the mesoscale sedimentation chamber (top) or a leading depth filter designed for white blood cell (WBC) capture (bottom). B. Cell capture results from the two devices using the Sysmex Blood analyzer as described above. C. Cell capture (blue) and flushing (red) efficiency from the device after capture within the sedimentation chamber (at various flow rates).

Extension to Rare Cell Capture (with syringe actuation): In one final test of the versatility of the device we decided to attempt to capture a low number of input cells. In this experiment we diluted pre-purified PBMCs to either 18,000 cells/mL or 250,000 cells/mL input. In addition, we ran the device through simple hand actuation of a syringe (syringe was connected to the plasma collection chamber in order to generate vacuum for running the device). Even without controlled syringe pump operation, in our single experiment with rare cells the device enabled capture of 7880/18000 input cells (with 74.8 % viability) at the lower concentration and 114,600/250,000 cells (with 97.6 % viability) at the higher concentration. This n=1 experiment needs to be repeated in further tests to determine the ability of the device to function in the capture of rare or dilute cells, but demonstrates the capability of running the device without external equipment (i.e. syringe pump).

S4 – Plasma Separation Efficiency

In applications focused on cell-free plasma analysis, it is useful to understand how device configuration and processing parameters affect the capture efficiency and level of dilution of the collected plasma. Since the sedimentation chamber is primed with buffer solution, there is always some level of plasma dilution, but this level varies with input volume as well as with the size of the sedimentation chamber. Reducing the volume of the sedimentation chamber reduces the required amount of initial priming buffer, and thereby increases the final concentration of plasma relative to buffer in the collection chamber. Since the size of the sedimentation chamber dictates the volume of cells that can be captured, the design of the system can be optimized to balance plasma dilution with the required blood processing capacity.

However, while plasma dilution is solely a function of device design (and sedimentation chamber size), plasma collection efficiency is not. This is due to the ability to add an additional volume of buffer to the input chamber (after the primary blood sample is run through the device), which will push/extract plasma trapped within the sedimentation chamber (leaving cells behind). In table 3 this is labelled as the Post-blood Buffer Flush. This flush results in more plasma collected from the sample (specifically, cell-free portions of the plasma), but an additional dilution of the collected plasma with buffer. Table 3 demonstrates how plasma collection efficiency and plasma dilution will vary with device design (with or without a Post-blood Buffer Flush).

The diagram in figure S4 illustrates how we arrived at the values in table S3. Step 1 depicts that initially the device is primed with a buffer solution (within the sedimentation chamber), prior to introduction of blood into the input chamber (step 2). In step 3, blood begins to run through the device and cells (and particulates) settle to the bottom of the collection chamber, while the non-cellular portion of the plasma (including cell-free nucleic acid) remain evenly distributed throughout the chamber. However, no plasma is initially collected, as the priming buffer is closest to the collection chamber and enters first. Next in step 4, once a blood volume equivalent to the sedimentation chamber volume has been run through the device plasma will begin entering the collection chamber (while the sedimented cells remain in the bottom). Plasma collection will continue in this step, until there is no blood sample remaining in the input chamber. In this case, if the blood sample is much smaller than the sedimentation chamber volume than a significant portion of plasma will be left behind (see the first two rows in table 3). However, even in this limiting input case, an addition buffer volume can be added to the input chamber (step 5) and run through the device to collect additional plasma (with little to no contamination from the sedimented cells).

We note that this simple volumetric calculation is limiting as diffusive mixing due to plug flow within the sedimentation chamber will alter the exact timing of the plasma initially reaching the collection chamber and the volume required for 100% plasma collection. However, our results within the text show that a large amount of cell-free nucleic acid can be collected using these steps and it is clear that plasma collection efficiency can be increased by simply running additional buffer through the system. In addition, we note that the rapid processing speeds within our device (0.5 mL/min and above) is dependent on cell trapping immediately upon hitting the bottom collection chamber surface (such that sedimentation of one “critical height” distance causes irreversible cell capture). However, again our data

throughout the text shows that this is practically feasible using the materials listed in the experimental section. We note that effective capture may be due to aggregation of cells (especially red blood cells which are known to aggregate at low shear rates); however, capture efficiencies were similar using the same device for both cells (data in the main text) and silica particles (data in table S1 and S2 above).

Initial Volume of Plasma in Blood Sample (mL)	Sedimentation Chamber Volume (mL)	Post-Blood Buffer Flush (mL)	Total Solution Collected (mL)	Actual Plasma Collected (mL)	% Plasma Concentration (Act. Plasma Collected/ Total Solution Collected)	% Plasma Recovery (Act. Plasma Collected/Initial Volume of Plasma in Blood Sample)
0.25	0.5	0	0.25	0	0%	0%
0.5	0.5	0	0.5	0	0%	0%
1	0.5	0	1	0.5	50%	50%
2	0.5	0	2	1.5	75%	75%
0.25	0.5	0.5	0.75	0.25	33%	100%
0.5	0.5	0.5	1	0.5	50%	100%
1	0.5	0.5	1.5	1	67%	100%
2	0.5	0.5	2.5	2	80%	100%
0.25	0.75	0.5	0.75	0	0%	0%
0.5	0.75	0.5	1	0.25	25%	50%
1	0.75	0.5	1.5	0.75	50%	75%
2	0.75	0.5	2.5	1.75	70%	88%
0.25	0.75	0.75	1	0.25	25%	100%
0.5	0.75	0.75	1.25	0.5	40%	100%
1	0.75	0.75	1.75	1	57%	100%
2	0.75	0.75	2.75	2	73%	100%

Table S3. Table demonstrating the theoretical plasma collection efficiency and plasma dilution after running a specified input blood volume through the device (left column). Each row gives the estimated collection parameter for specific device geometry and run parameters (i.e. sedimentation chamber volume and buffer flush volume).

Figure S4. An illustration of how the plasma collection efficiency and plasma dilution is dependent on device design (i.e. sedimentation chamber volume) and operation parameters (i.e. Post-blood Buffer Flush).